Synthesis and characterization of Y2O3:Eu3+ phosphors using the Sol–Combustion method

Article *in* Physica B Condensed Matter · April 2014

DOI: 10.1016/j.physb.2013.11.051

3 authors:

Abdub Guyo Ali
University of the Free State
6 PUBLICATIONS **19** CITATIONS
SEE PROFILE

Francis Dejene
University of the Free State
25 PUBLICATIONS **85** CITATIONS
SEE PROFILE

H. C. Swart
University of the Free State
528 PUBLICATIONS **3,327** CITATIONS
SEE PROFILE

Physica B 439 (2014) 181–184

Contents lists available at ScienceDirect

Physica B

journal homepage: www.elsevier.com/locate/physb

Synthesis and characterization of Y_2O_3:Eu^{3+} phosphors using the Sol-Combustion method

A.G. Ali [a,*], B.F. Dejene [a], H.C. Swart [b]

[a] Department of Physics, University of the Free State (QwaQwa Campus), Private Bag X13,Phuthaditjhaba ZA9866, South Africa
[b] Department of Physics, University of the Free State, P.O. Box 339, Bloemfontein ZA9300, South Africa

ARTICLE INFO

Available online 3 December 2013

Keywords:
Rare earth oxide
Combustion decomposition reaction
Y_2O_3

ABSTRACT

Y_2O_3:Eu^{3+} phosphor powders were prepared by the Sol-Combustion synthesis method using a sulfur-contained organic fuel in an ethanol–aqueous solution. The structural, morphological and optical properties of the as-prepared Y_2O_3:Eu^{3+} phosphors were obtained for different fuel to host ratios (S/Y molar ratios). The estimated grain sizes were calculated using the X-ray diffraction patterns were found to vary between 158–180 nm. The grain sizes were found to slightly decrease with the increase of the S/Y molar ratios. From photo luminescent spectra, the main emission peak arising from the $^5D_0 \rightarrow {}^7F_2$ transition was observed at 626 nm, while the weaker emissions at shorter wavelength values were ascribed to the $^5D_1$, $^5D_2 \rightarrow {}^7D_J$ ($J=1, 2, 3, \ldots$) transitions of Eu^{3+}. From these emission spectra it was clear that the S/Y molar ratios have significant effects on the maximum intensities and phosphorescence time of these phosphors.

1. Introduction

Global claim for phosphor materials as efficient sources of energy that can supply sustained competence is growing day by day. The phosphors are facing increased global challenges including high production of rare earth materials, environmental and recycling issues, and necessity to supply devices very quickly that may be outdated rapidly due to new technological developments arising in the industry and market. A number of applications have emerged in recent years that will change the future of the industry and new technologies like innovations and specialty phosphors are garnering increased attention. The primary drivers for growth are the expansion of key end-use applications including solid-state lighting and fluorescent lighting. Current research in technology is focused on new materials, novel phenomena, new characterization techniques and fabrication of devices. The manufacturing of the new generation of display equipment in recent years raised a stringent demand on the fluorescent materials [1]. Particular interest is focused on the high-brightness phosphors having sub-micrometer particle sizes. Conventional solid-state synthesis of phosphors followed by milling generally results in a dramatic decline of emission intensities for 1–3 μm size particles due to the defects introduced by crushing. Therefore, the wet-chemical methods seem to be an attractive alternative to the classical approach. The attempts to prepare fine powders of Y_2O_3:Eu^{3+}, perhaps the simplest oxide among industrially used phosphors, usually lead to broadening of the emission peaks and overall decrease of the luminescence performance [2,3]. Trivalent-europium-doped yttrium oxide (Y_2O_3:Eu^{3+}) is an important phosphor system extensively applied in color-television picture tubes owing to higher luminescent efficiency and the saturation degree in color. Y_2O_3, with a band gap of 5.8 eV can be considered as a large band gap semiconductor system [4]. In this paper we investigate how the structure, morphology and the luminescence intensities of these phosphors are affected by varying fuel to host ratios (S/Y).

2. Experimental details

2.1. Synthesis procedure

All the chemicals used for the preparation of the powders were of analytical grade. It includes yttrium nitrate ($Y(NO_3)_3 \cdot 6H_2O$) (Y), thiourea (NH_2CSNH_2), europium nitrate ($Eu(NO_3)_3 \cdot 6H_2O$), ethanol and distilled water. During the preparation of the micro-powders, thiourea (S) was used as a fuel. Y_2O_3:Eu^{3+} micro-powders were prepared as follows:

$Y(NO_3)_3 \cdot 6H_2O$, NH_2CSNH_2, $Eu(NO_3)_3 \cdot 6H_2O$, ethanol and distilled water were mixed in required stoichiometric ratios and dissolved by stirring using a magnetic stirrer for 5–10 min. The mixture was heated in an air tube furnace to ignition temperature of 400 °C. A white foamy product was obtained after the combustion reaction. Different S/Y molar ratios (1.8–4) were used to prepare the different phosphor samples.

* Corresponding author. Tel.: +27 58 718 5269; fax: +27 58 718 5444.
E-mail addresses: aliag@qwa.ufs.ac.za, aliabdub@gmail.com (A.G. Ali).

0921-4526/$ - see front matter © 2014 Published by Elsevier B.V.
http://dx.doi.org/10.1016/j.physb.2013.11.051

2.2. Characterization

The Photoluminescence (PL) spectra as well as decay curves for all the samples were investigated using a Cary Eclipse fluorescent spectrophotometer equipped with a 150 W xenon lamp at an excitation source with the slit of 1.0 nm and scan speed of 240 nm min^{-1}. To determine the average particle diameter and the phase of the samples, X-ray powder diffraction (XRD) spectra were measured with a D8 Bruker Advanced AXS GmbH X-ray diffractometer using Cu *Ka* radiation at a wavelength of 0.154056 nm, the size and morphology of the as-prepared particles were carried out by using a Scanning electron microscope (SEM), SHIMADZU SSX-550 SUPERSCAN.

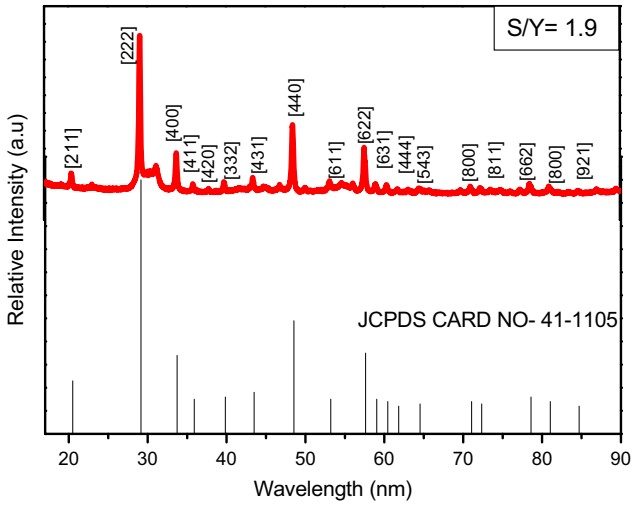

Fig. 1. Representative XRD pattern of one of the sample with a S/Y = 1.9 M ratio obtained by the Sol-Combustion method.

3. Results and discussion

3.1. Crystal structure

The XRD pattern of a representative as-prepared sample is shown in Fig. 1. All peaks can be perfectly indexed as the cubic phase with space group D_3d^3 (p^{3m}) and the cell parameter $a_0 = 10.60$ Å ($a = b = c$) is in good agreement with the standard Y_2O_3 JCPDS cards (No. 41- 1105). C_3 symmetry operation of Y^{3+} exists in the crystal, and no new crystal phase arose by doping with Eu^{3+}. The grain sizes ranging between 158 and 180 nm, were estimated by using the Scherrer's equation. In order to investigate if a marginal decrease in unit cell volume occurred; the crystallographic unit cell volume was determined by using the following equation:

$$\frac{1}{d^2} = \frac{h^2 + k^2 + l^2}{a^2}$$

It was observed that for the Y_2O_3 microstructures, there was a marginal decrease (-0.29%) in the crystallographic unit-cell that tends to contract due to the increase in surface area of the grains. This may lead to a decrease in the lattice constant. No peaks attributable to other types of oxides were observed in the XRD patterns, indicating the high purity of the phases obtained.

3.2. Morphology

The microstructures of the Y_2O_3:Eu^{3+} phosphors were studied with the SEM images as presented in Fig. 2. It can be seen from the images that the samples' morphology has changed from a bulky structure to define micro particles with an increase in the molar ratio. With the increase in the S/Y molar ratio the particles seem to agglomerate to form more definite micro structures. This morphology seems to be influenced by the composition of the molar

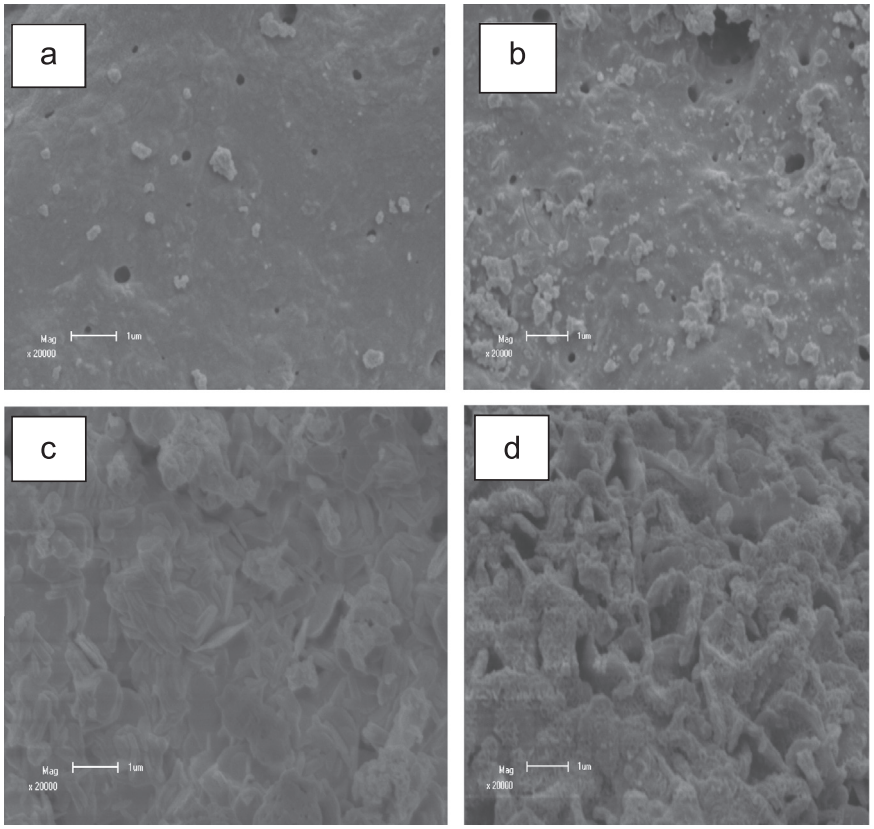

Fig. 2. The SEM images of the Y_2O_3:Eu^{3+} with (a) 1.9 (b) 2.0 (c) 2.5 and (d) 4 S/Y molar ratios. 10 μm field of view.

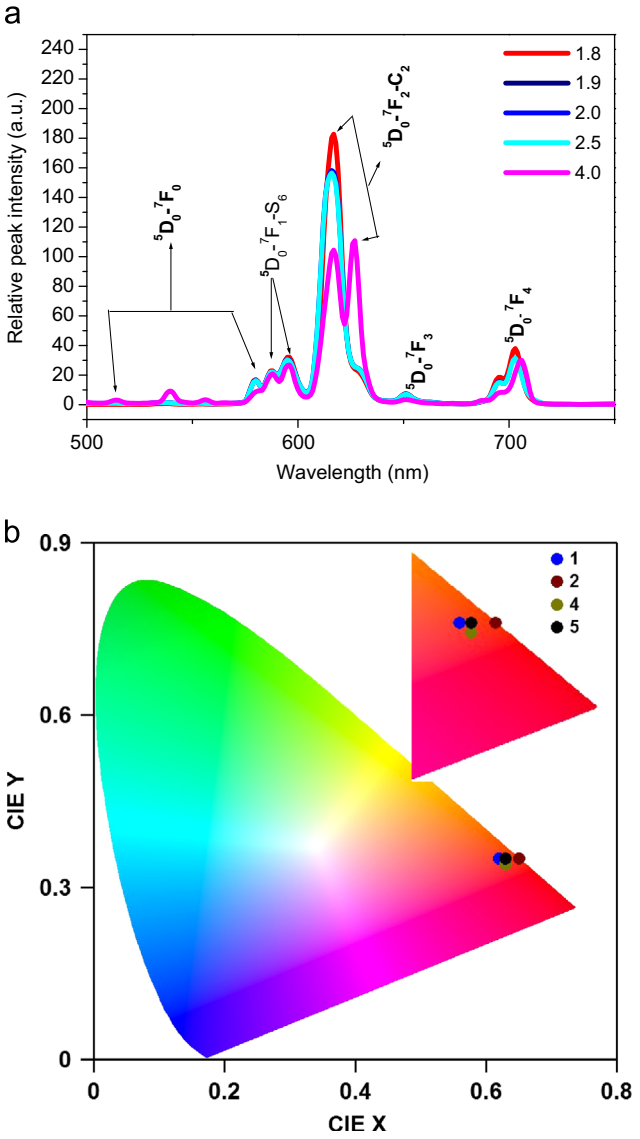

Fig. 3. (a): Emission spectra of the different S/Y molar ratio Y_2O_3:Eu^{3+} phosphor excited at 260 nm obtained by the Sol-Combustion method. (b) CIE coordinate diagram of the different emissions as indicated.

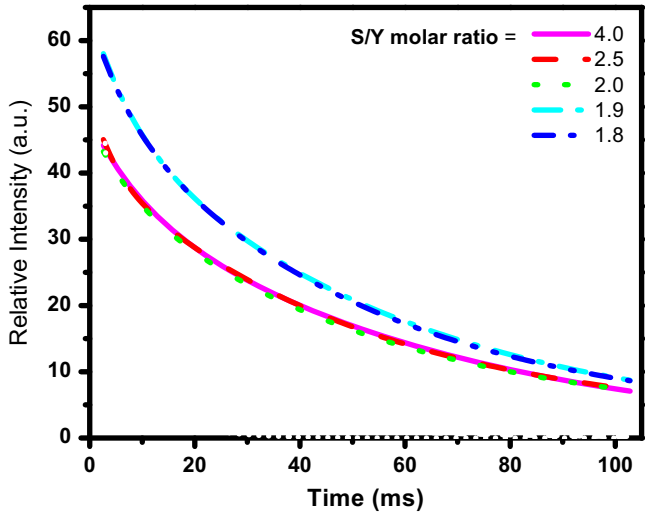

Fig. 4. The decay curve of the Y_2O_3:Eu^{3+} phosphor.

ratios. This current method also allowed obtaining agglomerates of controlled size since synthesis time can be controlled; this being an important advantage comparing with other methods [1,5,8]. Further on, the more defined morphology of the particles as evident in Fig. 2(d) benefits the emissivity of materials for phosphor applications, as is reported elsewhere [6,8]. An additional advantage of agglomerates is its excellent fluidity [11], which is beneficial for the elaboration of pressed bodies.

3.3. Photoluminescence

Upon excitation, Eu^{3+} doped systems indicate many Stark energy levels in the visible region. In particular, luminescence transitions corresponding to the $^5D_0 \rightarrow {}^7F_J$ manifold in the orange–red region are of practical significance [9]. Fig. 3(a) shows the emission spectrum of the Eu^{3+} ion doped in aY_2O_3 matrix with different S/Y molar ratios. The emission observed in the 514–700 nm range is ascribed to the well-known Eu^{3+} $^5D_0 \rightarrow {}^7F_J$ (J=0, 1, 2, 3 and 4) transitions. There are three groups of distinctive emission peaks between 580 and 626 nm, which are related to

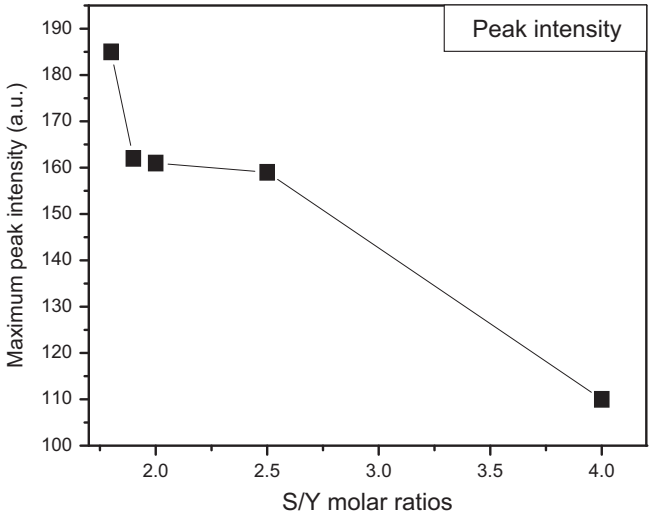

Fig. 5. Effect of S/Y molar ratios on the intensity of the broad PL peaks and corresponding emission wavelength.

Table 1
The average grain size of the synthesized Y_2O_3:Eu^{3+} nanoparticles as a function of S/Y molar ratio.

Average grain sizes as a function of S/Y molar ratios				
S/Y ratio	⟨2 2 2⟩	⟨4 0 0⟩	⟨4 4 0⟩	⟨6 2 2⟩
1.8	172	172	175	177
1.9	178	178	179	180
2	178	178	179	180
2.5	151	151	158	164
4	150	152	155	154

Table 2
Decay constants for the fitted decay curves of the phosphor powders with different S/Y molar ratios.

S/Y	1.8	1.9	2	2.5	4
Components					
Fast (τ1)	1.3715	1.3656	1.3647	1.3598	1.3579
Medium (τ2)	1.4588	1.4571	1.4537	1.4499	1.3989

the $^5D_0 \rightarrow {}^7F_J$ (J=0, 1, 2) transitions of Eu^{3+}, respectively. The strongest emission peak near 616 nm corresponding to forced electron dipole transition of Eu^{3+} is due to the $^5D_0 \rightarrow {}^7F_2$ transition in C_2 symmetry for Eu^{3+} incorporated in Y_2O_3, which is hypersensitive to environmental effects [6]. In addition, there are other energy transitions of Eu^{3+} corresponding to $^5D_0 \rightarrow {}^7F_0$ (515–580 nm), $^5D_0 \rightarrow {}^7F_1$ (586–597 nm) and $^5D_0 \rightarrow {}^7F_2$ (616–629 nm) in the luminescence spectra. In the cubic Y_2O_3 there are two crystallographic sites, one with C_2 symmetry and the other with S_6 symmetry. Therefore, it can be concluded that the Eu^{3+} ions replace Y^{3+} ions and occupy both the C_2 and S_6 symmetries because the emissions assigned to such symmetries were observed (Fig. 3(a)). Compared with $^5D_0 \rightarrow {}^7F_2$ transition, intensity of $^5D_0 \rightarrow {}^7F_1$ transition corresponding to the orange color is much lower, which makes Y_2O_3:Eu^{3+} a purer red phosphor.

At S/Y=1.8 the phosphors have a red emission intensity that was the strongest due to the dominance of the $^5D_0 \rightarrow {}^7F_2$ transition. At the S/Y= 4 M ratio the $^5D_0 \rightarrow {}^7F_2$ transition peak splitting has also occurred. Therefore, to have some insights of various luminescence transitions of Eu^{3+} doped in a matrix, this transition can be used as an internal standard [7,9,10]. Relative intensity of the hypersensitive transition with respect to the magnetic dipole transition as internal standard would give an idea on the transition strength of the hypersensitive transition.Fig. 4

In order to investigate the effect of the S/Y molar ratios on the maximum intensity of the phosphors, a graph of maximum peak intensity versus various molar ratios was plotted as shown in Fig. 5. The plot indicates that the maximum peak intensities were higher at lower S/Y ratios (S/Y=1.8–2.5). It drops drastically for the higher molar ratio of S/Y=4. The total brightness, however, was still the same, if the splitted peaks areas of the $^5D_0 \rightarrow {}^7F_2$ transition are added; only a slight change in color was obtained as indicated by the coordinates on the International Commission on Illumination (CIE) diagram, Fig. 3(b).

3.4. Afterglow decay curves of the red phosphors

The afterglow properties of samples with different S/Y ratios were compared, as shown in Fig. 4. It can be seen that afterglow origin of the sample of S/Y=1.8 and 1.9 has the highest afterglow, while the sample with the ratio of S/Y=4.0 has the lowest afterglow. Thus, the ratio S/Y=1.9 was taken as the optimum. The decay times of the phosphor can be estimated by using the following double exponential equation: Table 1

$$I = A_1 \exp(-t/\tau 1) + A_2 \exp(-t/\tau_2)$$

where I is the phosphorescence intensity, A_1, and A_2, are constants, t is time, τ_1 and τ_2, are decay times for exponential components, respectively. The fitting results of the parameters t_1 and t_2 are listed in Table 2 below.

4. Conclusion

A very simple and efficient chemical route to prepare a promising afterglow red phosphor by the Sol-Combustion synthesis is presented. Ethanol has the effect of decreasing the water needed, hence simplifying the experimental procedure by dissolving rare earth nitrate and sulfur-contained organic fuel into an even solution. This prompts the formation of rare earth oxide by igniting first during heating that lead to a combustion decomposition reaction. Y_2O_3:Eu^{3+} microcrystalline structures were obtained using thiourea as the organic fuel. The increase in the ratios of fuel to the host decreased the grain size and the maximum PL intensity of the phosphors.

Acknowledgment

The authors would like to acknowledge the National Research Foundation (NRF) and the University of the Free State (UFS) for financial support.

References

[1] K. Narita, Phosphor Handbook, CRC Press LLC, Boca Raton, FL, 1999.
[2] M.R. Royce, US Patent no. 3418, vol. 246, 1968.
[3] S.H. Cho, Y.S. Yoo, J.D. Lee, J. Electrochem. Soc. 145 (1998) 1017.
[4] M. Mikami, A. Oshiyama, Phys. Rev. B 57 (1998) 8939.
[5] L. Spanhel, M.A. Anderson, J. Am. Chem. Soc. 113 (1991) 2826.
[6] A. Eric, M. Eulenkamp, J. Phys. Chem. B 102 (2002) 5566.
[7] D.C. Reyolds, D.C. Look, B. Jogai, H. Mokoc, Solid State Commun. 101 (1997) 643.
[8] M. Liu, A.H. Kitai, P. Mascher, J. Lumin. 54 (1992) 35.
[9] Z.W. Jin, Y.Z. Yoo, T. Sekiguchi, T. Chikyow, H. Ofuchi, H. Fujioka, M. Oshima, H. Koinuma, Appl. Phys. Lett. 83 (2003) 39.
[10] X.T. Zhang, Y.C. Liu, J.Y. Zhang, Y.M. Lu, D.Z. Shen, X.W. Fan, X.G. Kong, J. Cryst. Growth 80 (2003) 254.
[11] H.J. Lee, S.Y. Jeong, C.R. Cho, C.H. Park, Appl. Phys. Lett. 81 (2002) 4020.